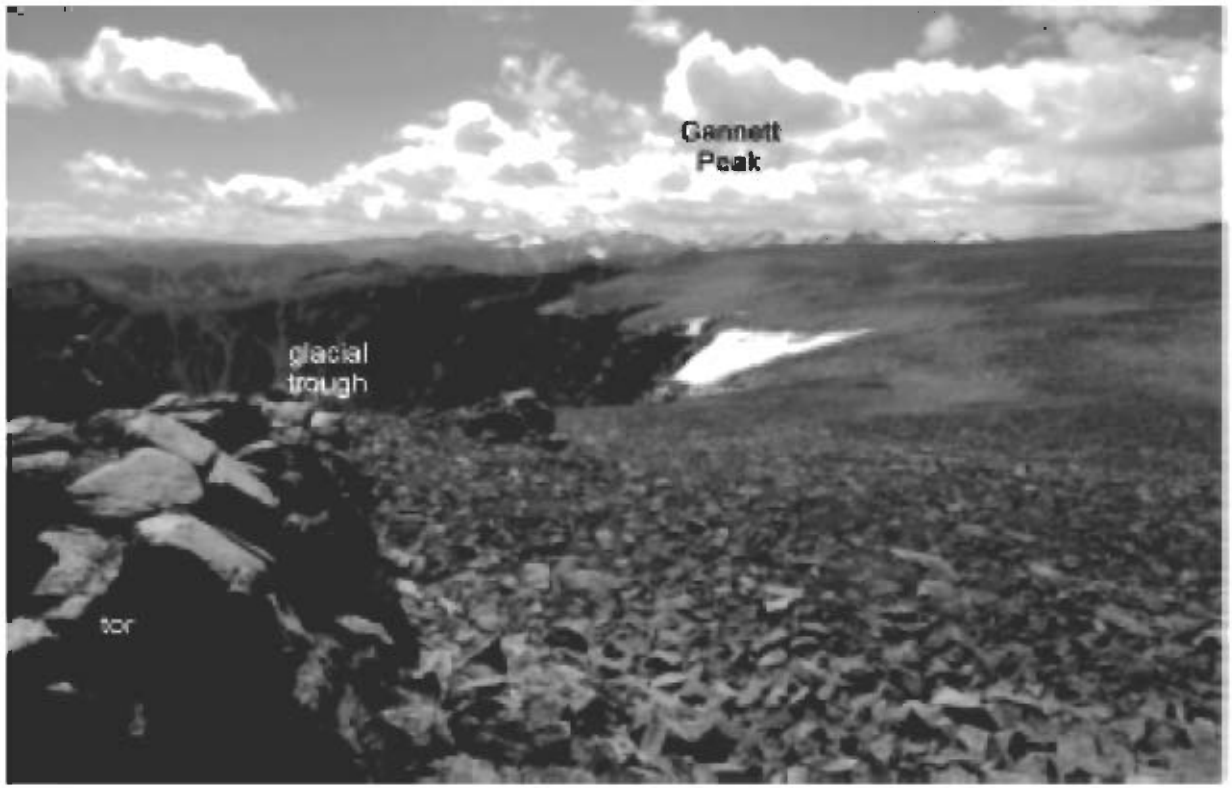

Fig. 2. View roughly southward from edge of bedrock tor on Goat Flat, with human figure for scale. Total relief of the tor is ~ 15 m. The tor adorns the crest of Goat Flat and, in this instance, is surrounded by a blockfield. Note large size of joint-bounded blocks on the tor. Goat Flat, at roughly 3500 m, is representative of numerous high surfaces. Gannett Peak on the crest of the range is on the horizon. A cross-section of the surface perpendicular to the trend of the ridge is very smooth (see Fig. 3), but drops abruptly into the adjacent glacial trough. Half-width of the surface is ~ 300 m. Note bedrock edge of the surface and extension of the smooth surface onto peninsulas jutting into the glacial trough. Where visible along this edge, the regolith is only about 1 m thick.

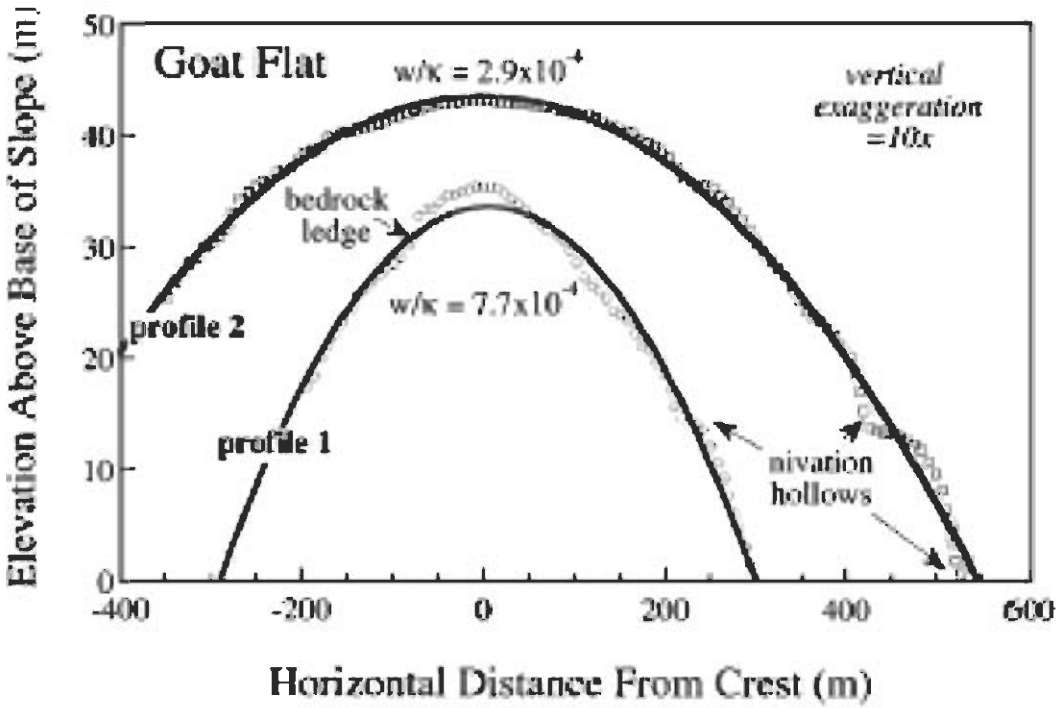

Fig. 3. Topographic profiles of an example of these high surfaces on Goat Flat in the Wind River Range. Profiles are hand-leveled and are separated by about 300 m along the crest of the surface, near photograph in Fig. 2. The only major deviations from the smooth profile are associated with nivation hollows on the flanks of the ridge. Only one, 2-m-tall bedrock ledge was encountered; otherwise, the entire surface was regolith-mantled. Curves are best-fitting parabolas, $z = z_{max} - (w/2\kappa)x^2$, are shown for each profile, where z_{max} is the maximum elevation of the profile. The ratio of regolith production rate to transport efficiency (w/κ, in m^{-1}) may be deduced from the curvature of the surface (see text for explanation).

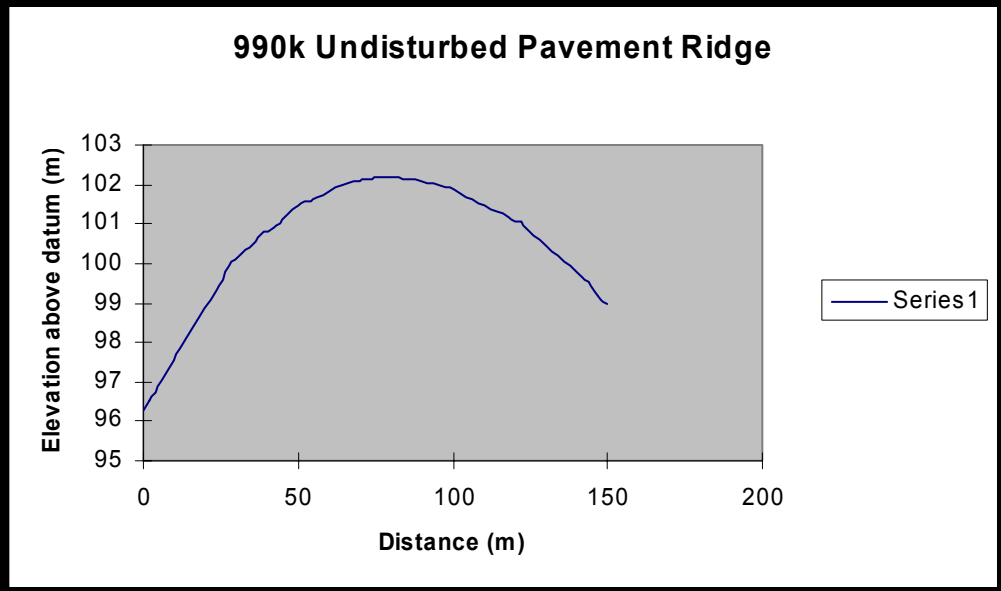
990k Undisturbed Pavement Ridge
Elevation above datum (m)
103
102
101
100
99
98
97
96
95
0
50
100
150
200
Distance (m)
Series1

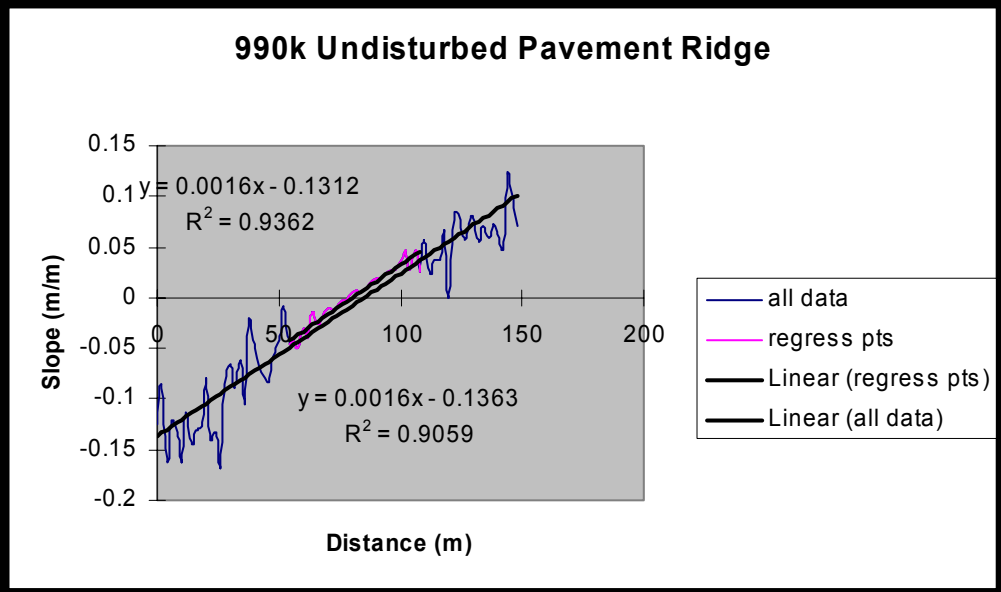
990k Undisturbed Pavement Ridge
Slope (m/m)
0.15
0.1
0.05
0
-0.05
-0.1
-0.15
-0.2
y = 0.0016x - 0.1312
R2 = 0.9362
y = 0.0016x - 0.1363
R2 = 0.9059
0
50
100
150
200
Distance (m)
all data
regress pts
Linear (regress pts)
Linear (all data)

KENNETH L. PIERCE
STEVEN M. COLMAN

Geological Society of America Bulletin, v. 97, p. 869–885, 15 figs., 5 tables, July 1986.

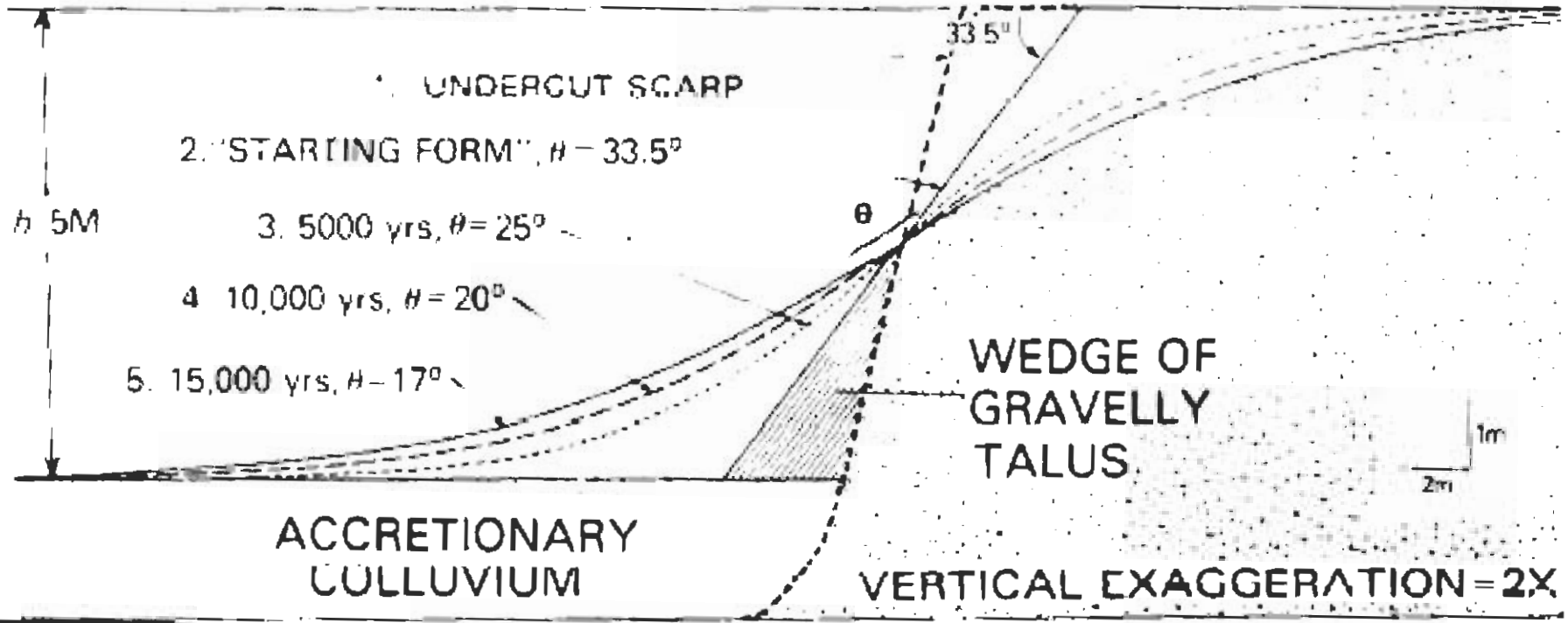

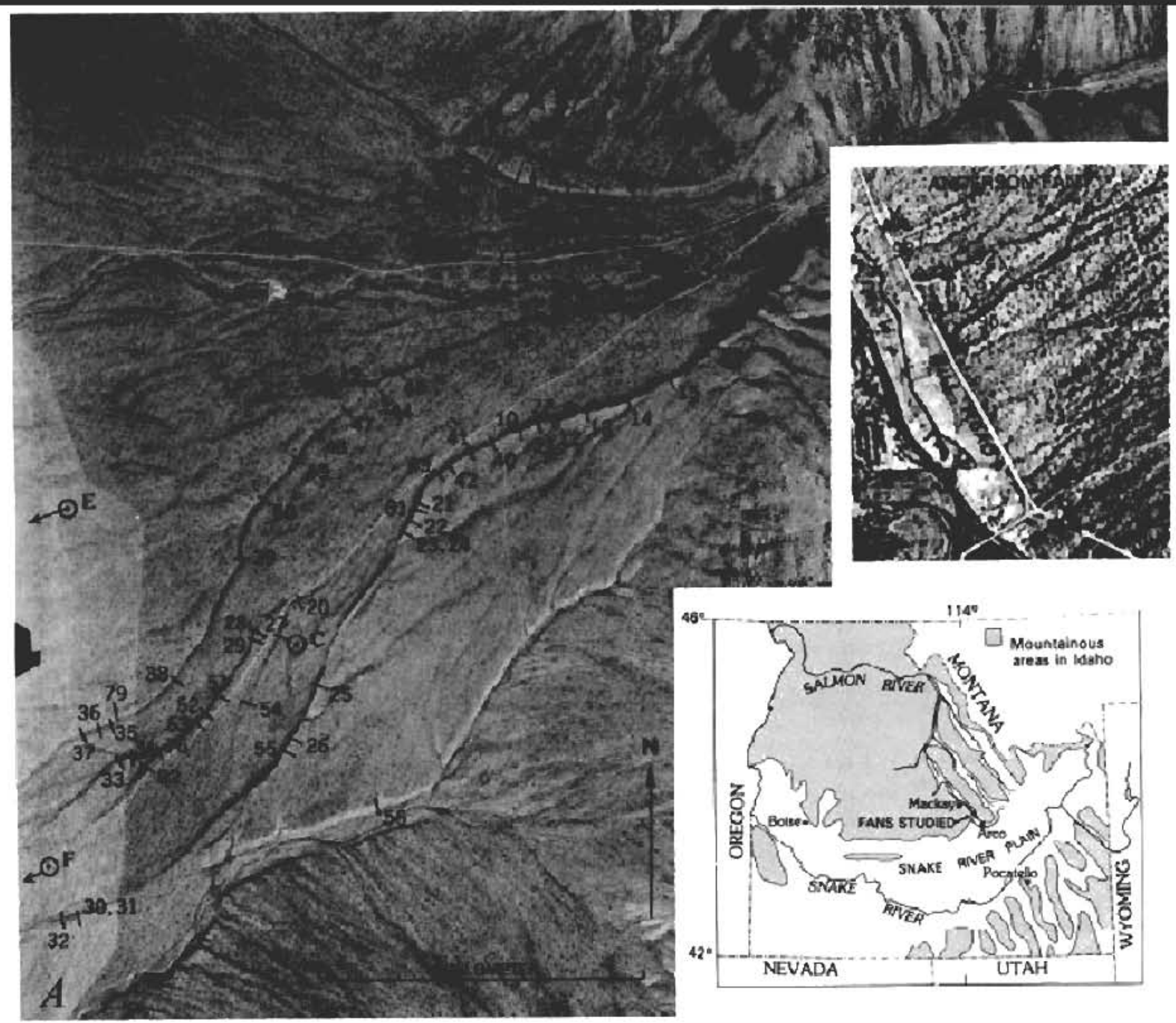
E
F
C
N
A
Mountainous areas in Idaho
SALMON RIVER
MONTANA
OREGON
WYOMING
NEVADA
UTAH
Boise
Pocatello
Arco
FANS STUDIED
SNAKE RIVER PLAIN
SNAKE RIVER
46°
114°
42°

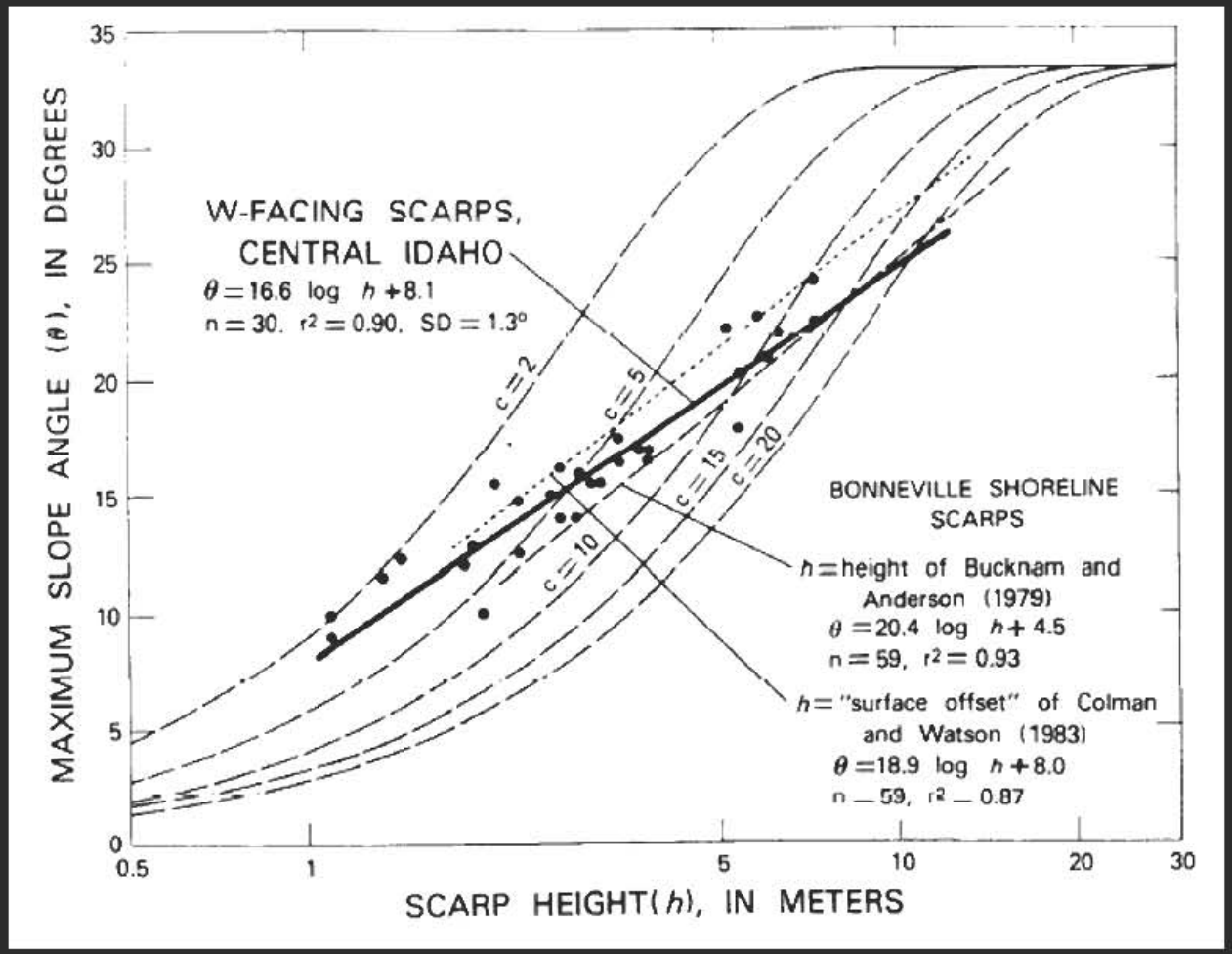
MAXIMUM SLOPE ANGLE (θ), IN DEGREES
SCARP HEIGHT(h), IN METERS
0
5
10
15
20
25
30
35
0.5
1
5
10
20
30
W-FACING SCARPS,
CENTRAL IDAHO
θ = 16.6 log h + 8.1
n = 30, r² = 0.90, SD = 1.3°
c = 2
c = 5
c = 10
c = 15
c = 20
BONNEVILLE SHORELINE SCARPS
h = height of Bucknam and Anderson (1979)
θ = 20.4 log h + 4.5
n = 59, r² = 0.93
h = "surface offset" of Colman and Watson (1983)
θ = 18.9 log h + 8.0
n = 59, r² = 0.87

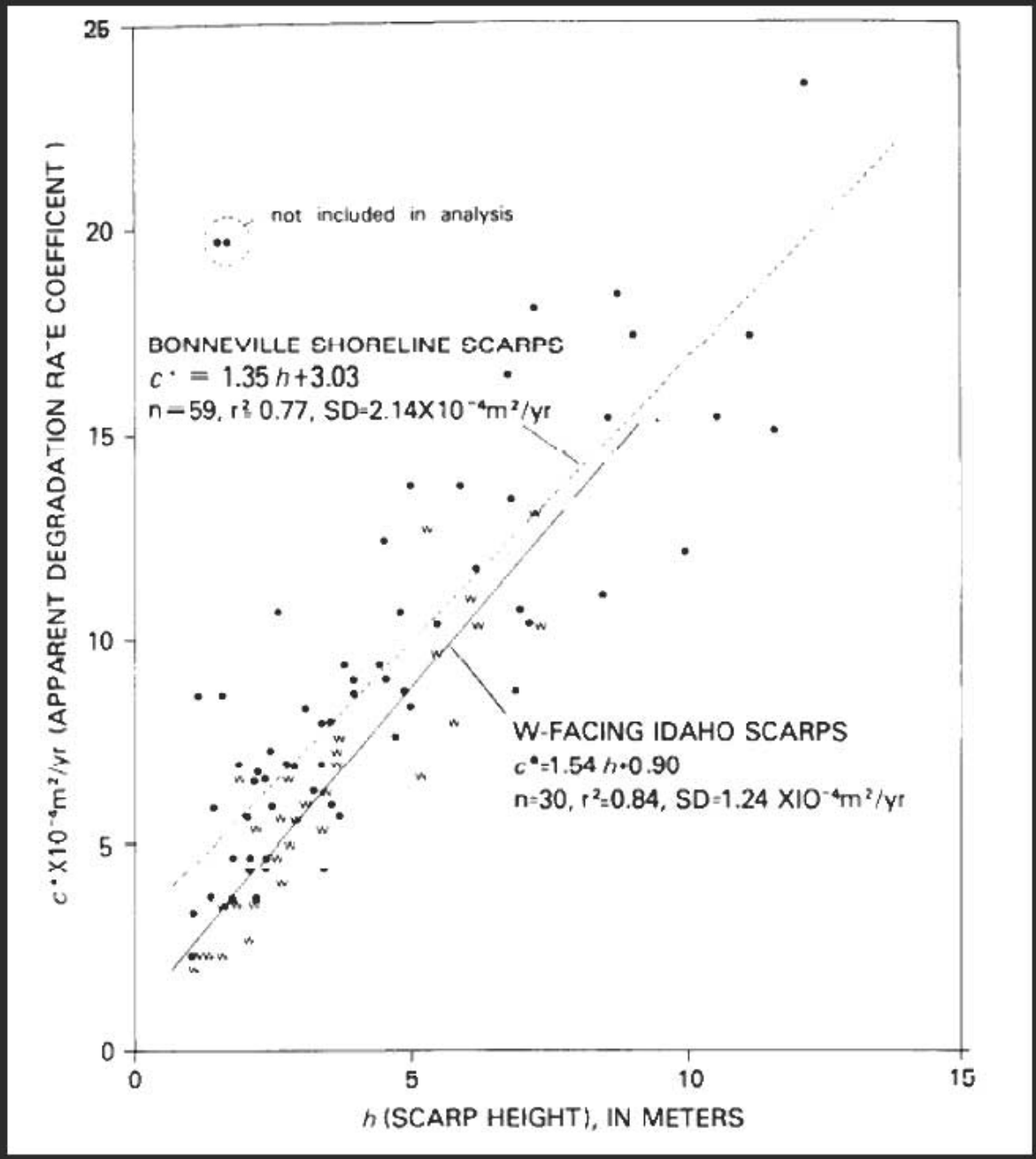
not included in analysis
BONNEVILLE SHORELINE SCARPS
$c^* = 1.35\,h + 3.03$
n=59, r² 0.77, SD=2.14X10⁻⁴m²/yr
W-FACING IDAHO SCARPS
$c^* = 1.54\,h + 0.90$
n=30, r²=0.84, SD=1.24 XIO⁻⁴m²/yr
c* X10⁻⁴m²/yr (APPARENT DEGRADATION RATE COEFFICENT)
h (SCARP HEIGHT), IN METERS
0
5
10
15
20
25

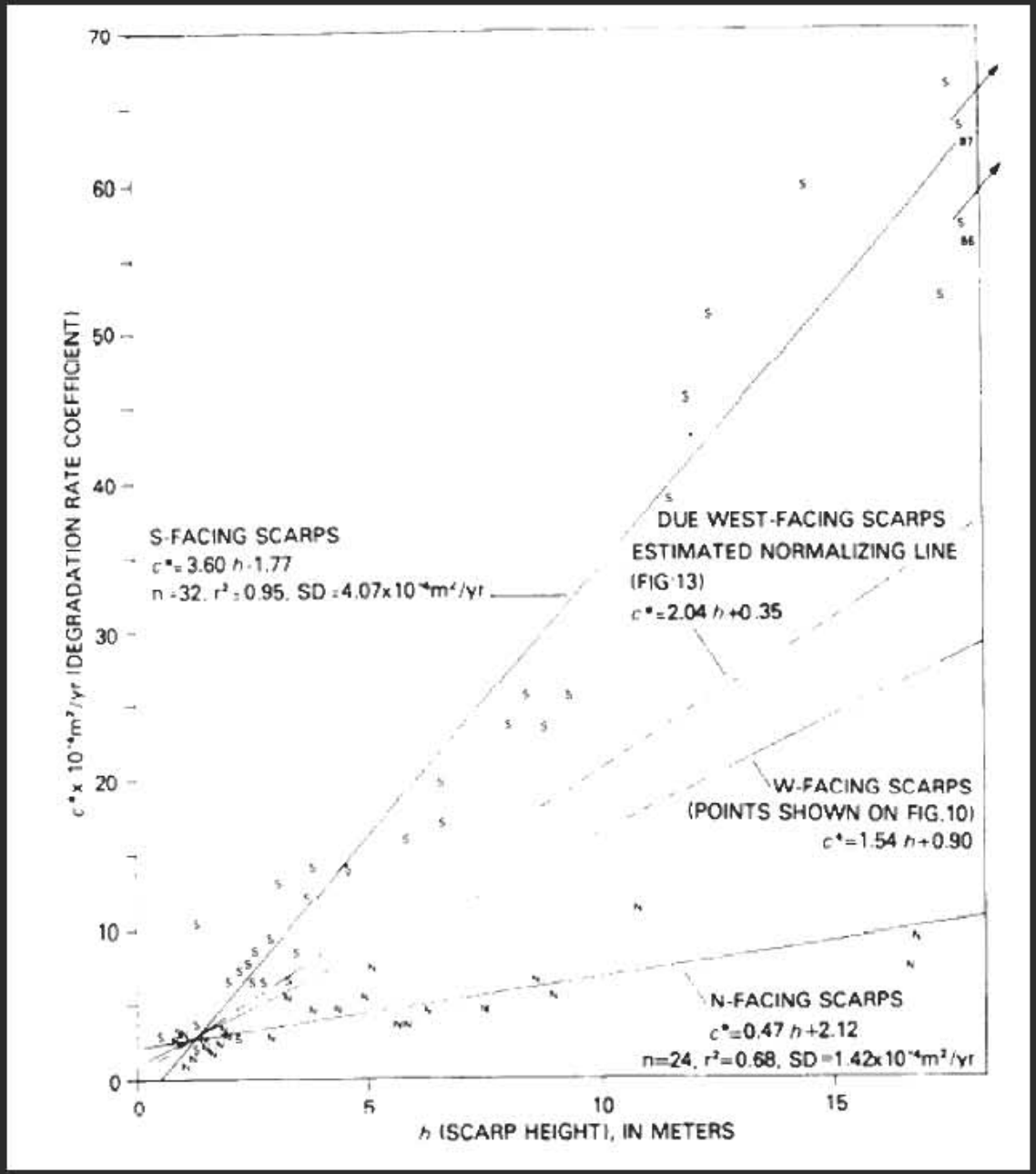
70
60
50
40
30
20
10
0
0
5
10
15
c^* x $10^{-4}m^2/yr$ (DEGRADATION RATE COEFFICIENT)
h (SCARP HEIGHT), IN METERS
S-FACING SCARPS
$c^* = 3.60\ h - 1.77$
$n = 32,\ r^2 = 0.95,\ SD = 4.07 \times 10^{-4} m^2/yr$
DUE WEST-FACING SCARPS
ESTIMATED NORMALIZING LINE
(FIG. 13)
$c^* = 2.04\ h + 0.35$
W-FACING SCARPS
(POINTS SHOWN ON FIG. 10)
$c^* = 1.54\ h + 0.90$
N-FACING SCARPS
$c^* = 0.47\ h + 2.12$
$n = 24,\ r^2 = 0.68,\ SD = 1.42 \times 10^{-4} m^2/yr$

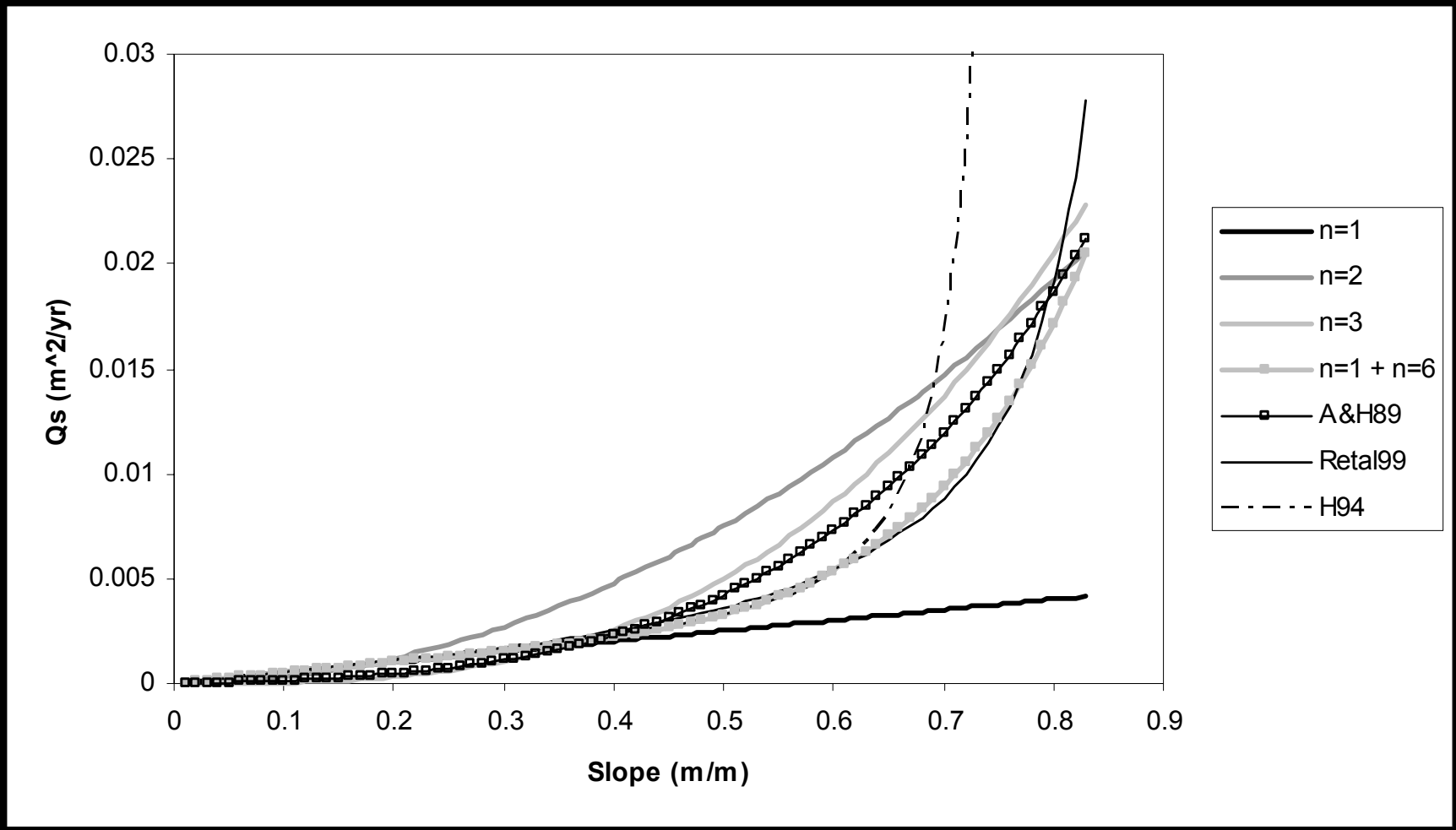
0.03
0.025
0.02
0.015
0.01
0.005
0
Qs (m^2/yr)
0
0.1
0.2
0.3
0.4
0.5
0.6
0.7
0.8
0.9
Slope (m/m)
n=1
n=2
n=3
n=1 + n=6
A&H89
Retal99
H94

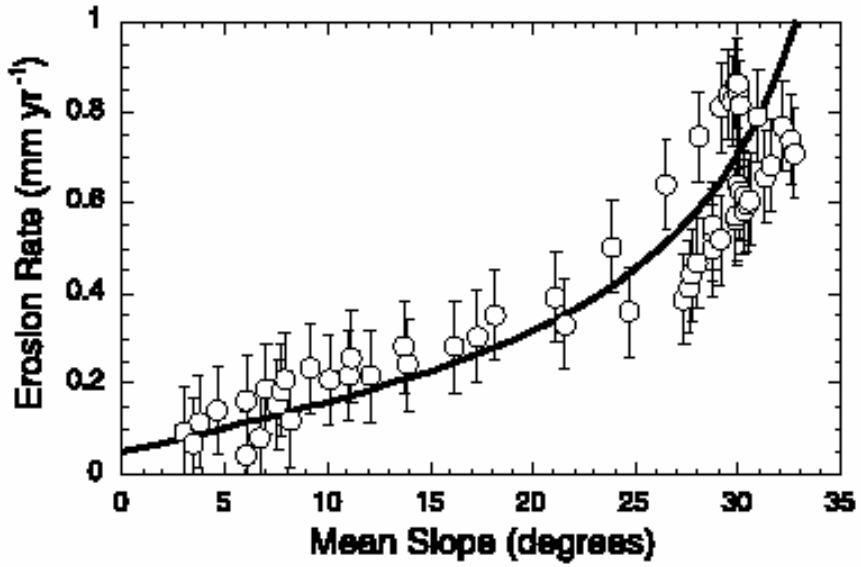

Fig. 1. Plot of long-term erosion rate versus mean slope for a transect across the Olympic Mountains. Erosion rate data are from low-temperature thermochronometry [39]. Mean slope values were determined for a 10-km-diameter area from a composite 10-m-grid DEM of the range around points spaced every 2 km along a transect across the range beginning from 47.5335°N., 235.6463°W. Solid line represents model fit using Eq. 1 with $E_0 = 0.05$ mm yr^{-1}, $K = 0.6$ mm yr^{-1}, and $S_c = 40°$. Error bars represent an uncertainty in erosion rates of 0.1 mm yr^{-1}.

$$E = E_0 + \frac{KS}{[1-(S/S_c)^2]}$$

Note: K not the diffusion constant
This is an “analogous expression” for erosion rate

Cosmogenic nuclides, topography, and the spatial variation of soil depth

Arjun M. Heimsath [a,*], William E. Dietrich [a], Kunihiko Nishiizumi [b], Robert C. Finkel [c]

Geomorphology 27 (1999) 151–172

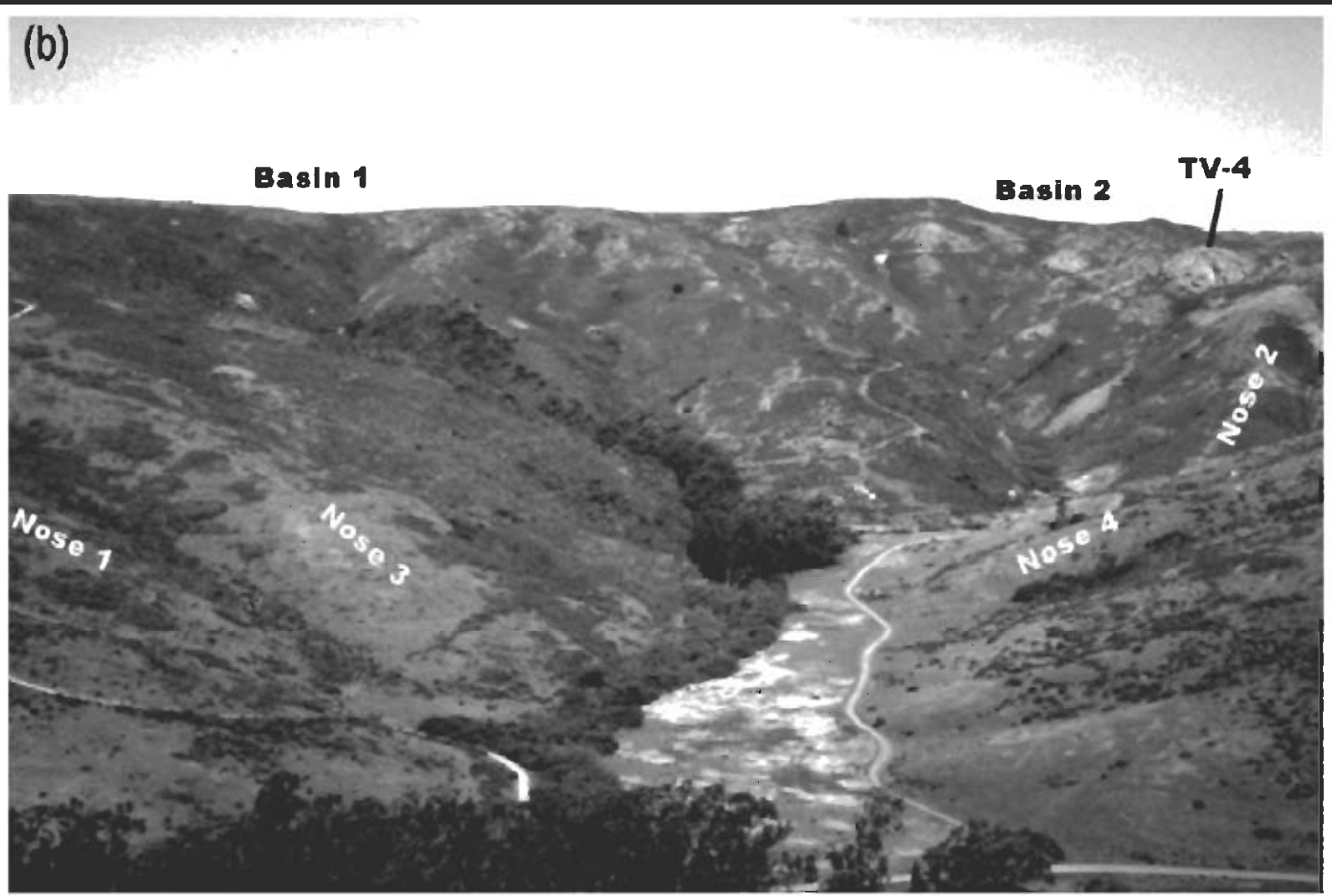

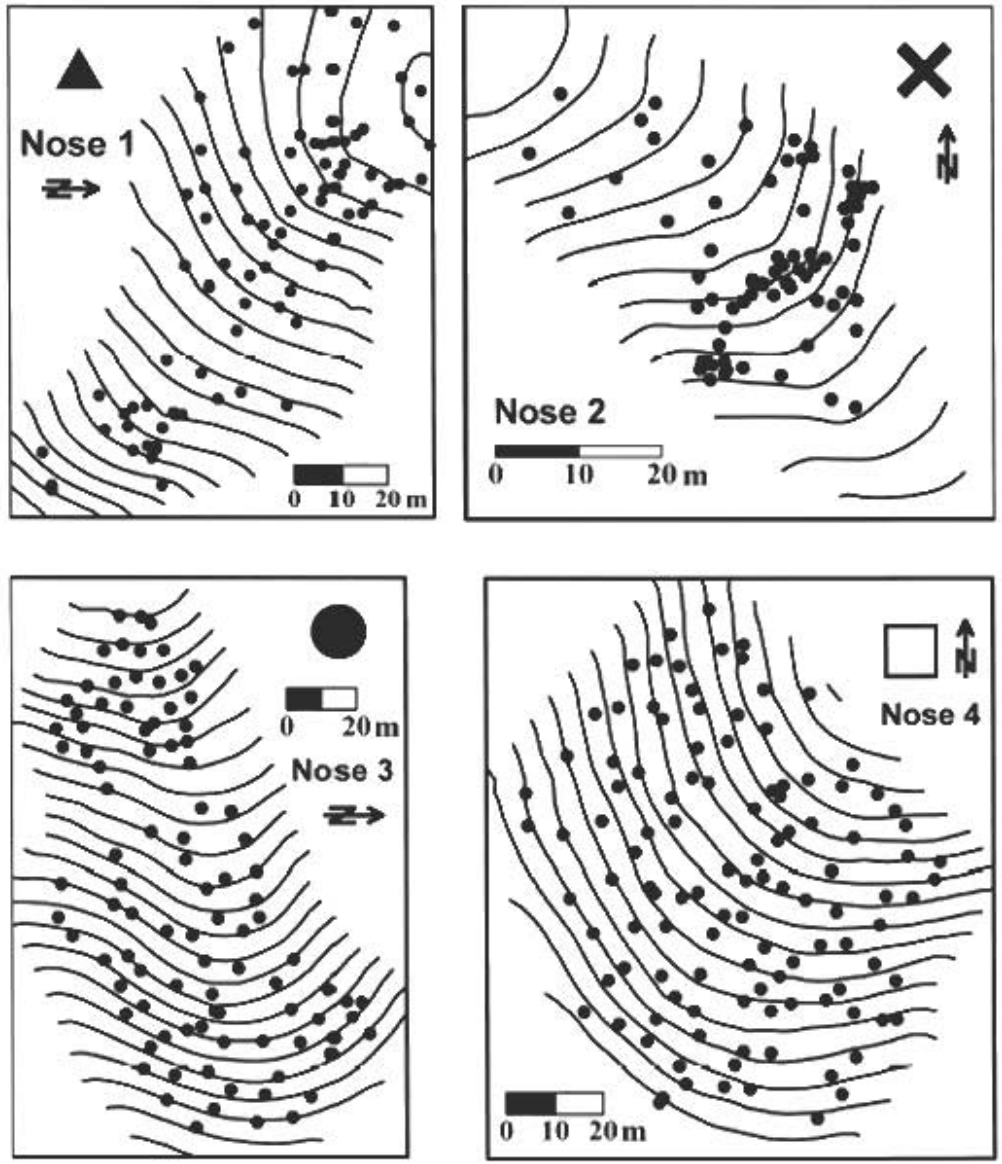

Fig. 5. The four noses surveyed for our curvature analyses are located on Fig. 3 inset map with the upper-corner symbols. We surveyed the topography at about 1–3 m resolutions and the 2 m contour lines shown here are drawn from 3.5 m grids generated by a *Kriging* interpolation scheme. Dots on the noses show locations of the depth measurements from either auger holes or pits and are equivalent to the large dot on Fig. 3.

Curvature ~ erosion rate vs soil depth

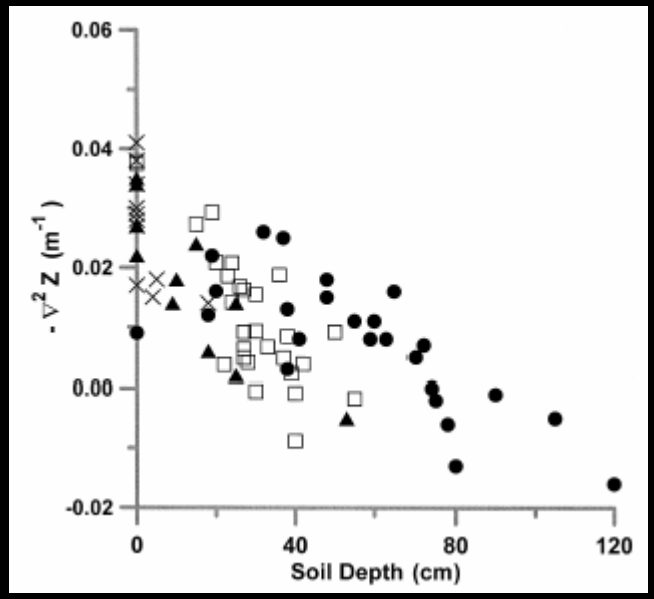

Cosmogenic production rate vs soil depth

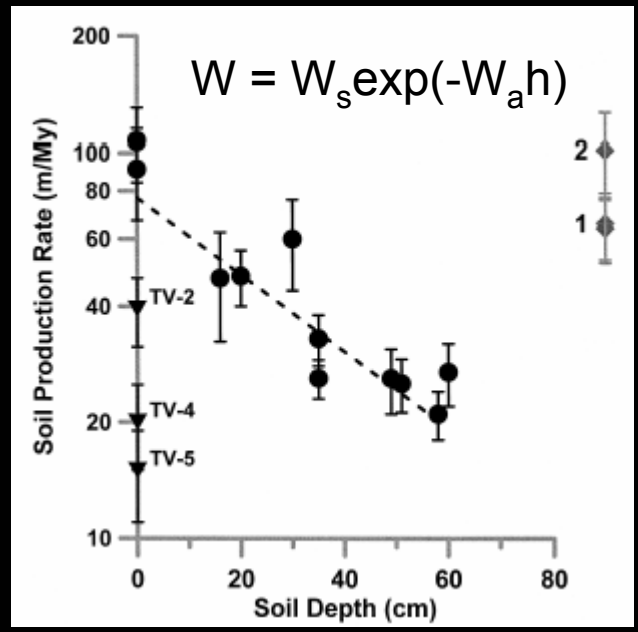

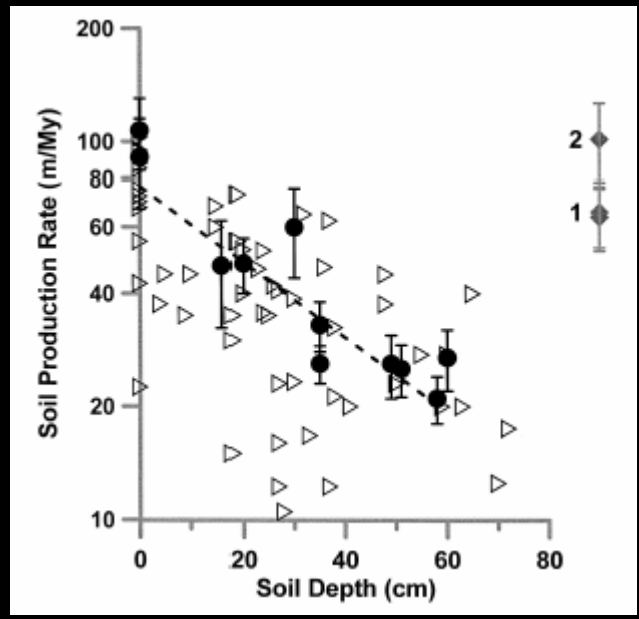

K = 5e-3 m^2/yr;
Independent estimates

Diffusion-law vs Cosmogenic production rate as function of soil depth

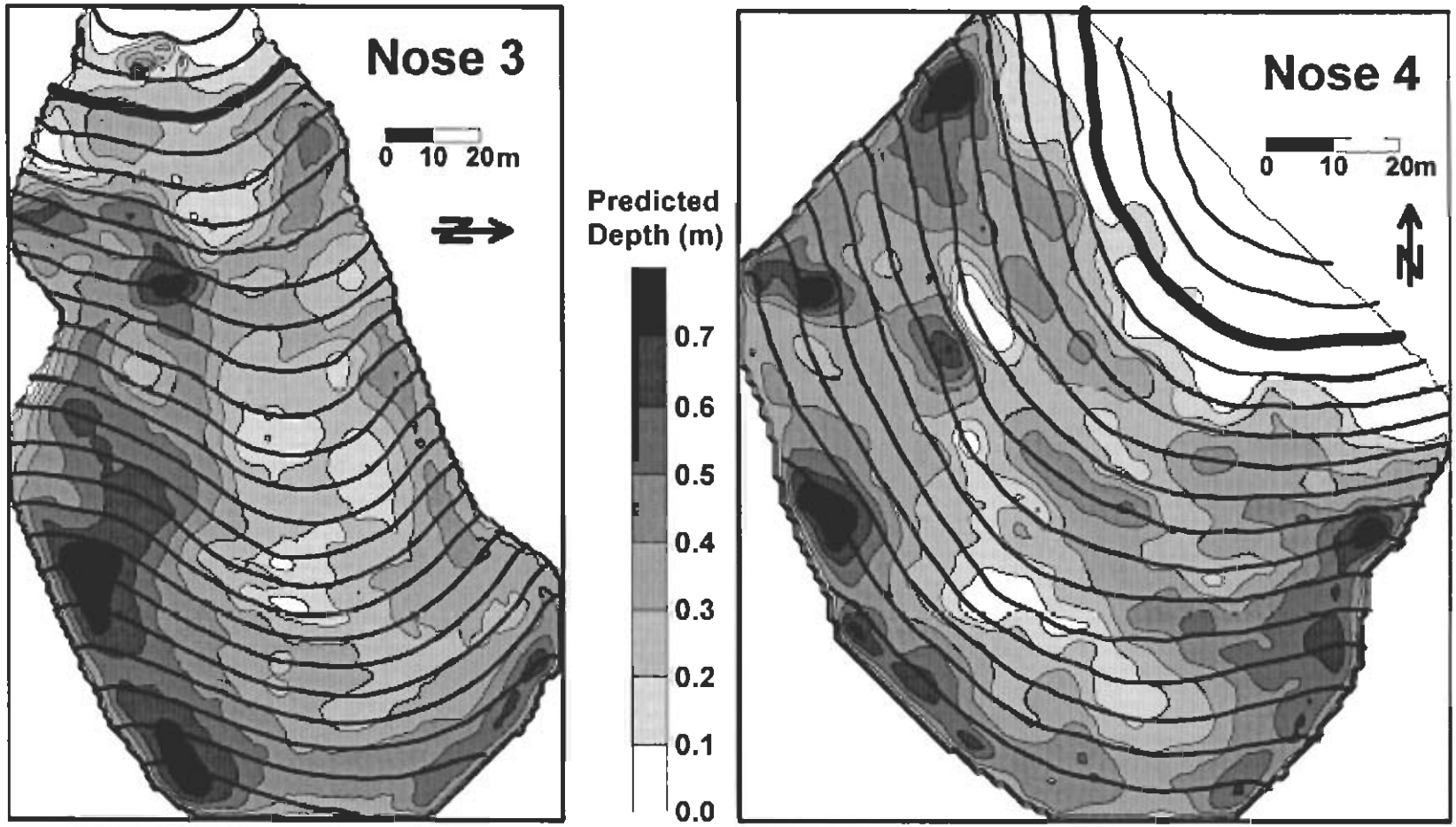

Fig. 9. Predicted depths of soil, in m, after 6000 years of running the soil model with 10-year time steps on all four surveyed noses. These predicted depths are determined using the exponential fit to the data here, shown in Fig. 7, as the function of soil production. Boundary conditions are explained in the text and initial soil thickness is zero. Topographic contour lines are drawn at 2 m, and are the same as Fig. 5. The thickened contour line near the top of each nose shows the cut-off elevation above which we treated predicted depths as upper-boundary artifacts and did not compare them to our observed depths in the area.

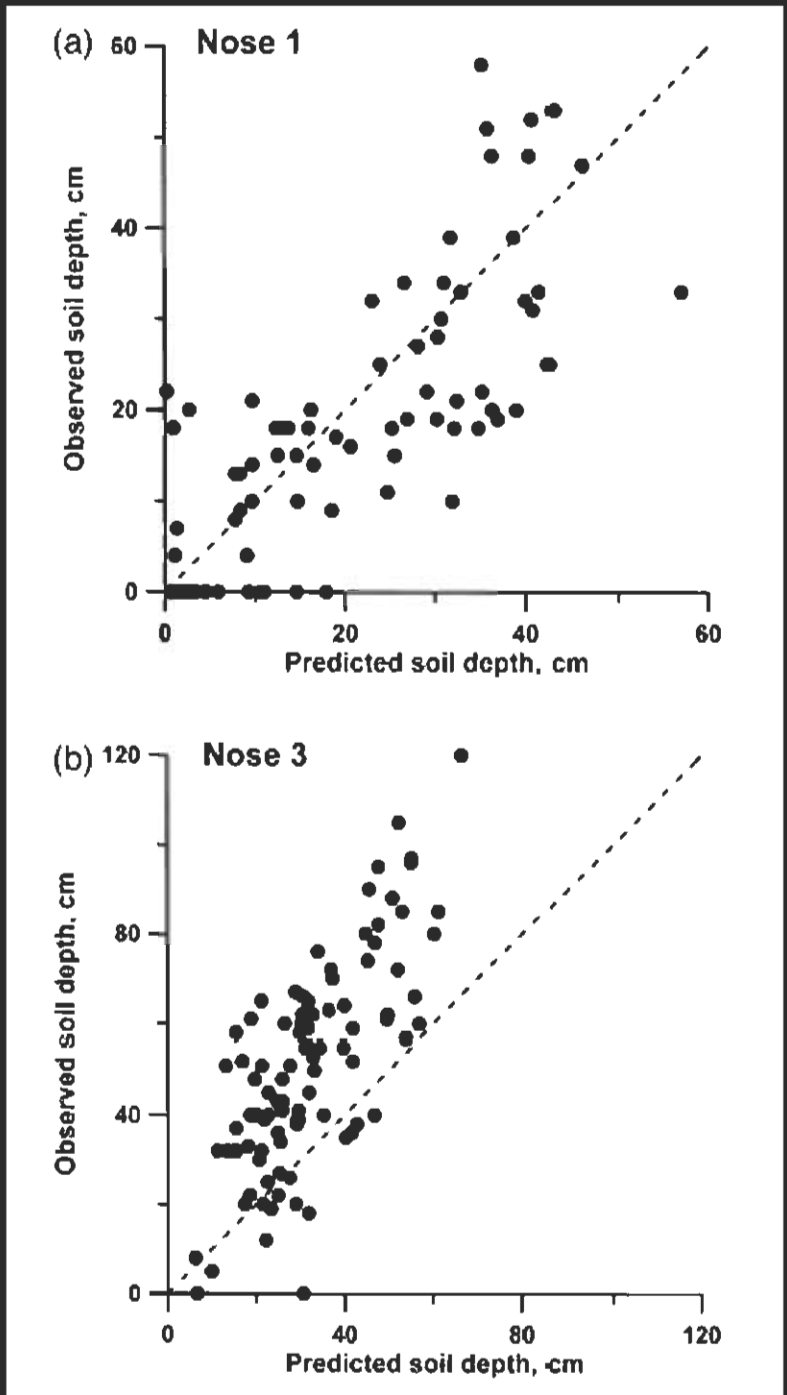
(a)
Nose 1
Observed soil depth, cm
Predicted soil depth, cm
0
20
40
60
(b)
Nose 3
Observed soil depth, cm
Predicted soil depth, cm
0
40
80
120

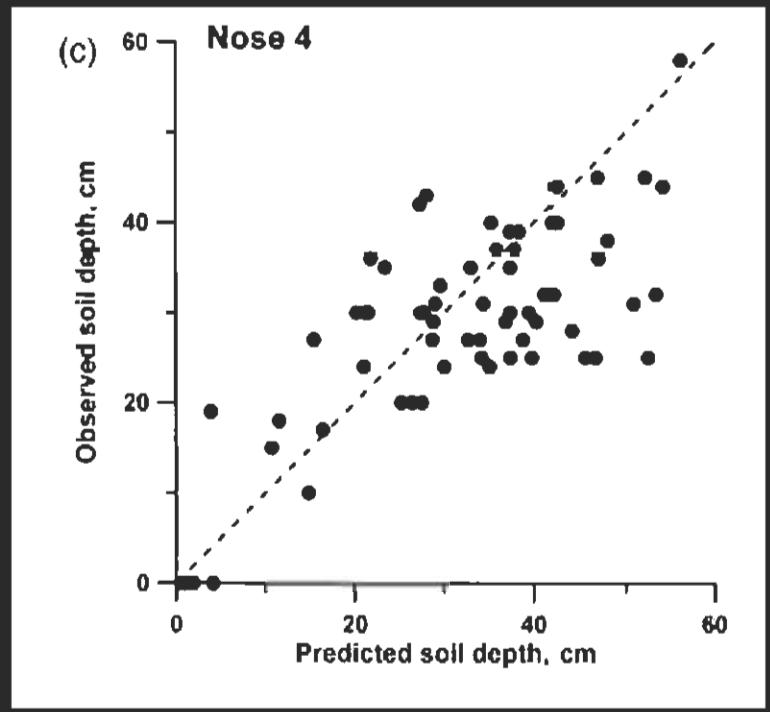
(c)
Nose 4
Observed soil depth, cm
Predicted soil depth, cm
0
20
40
60

Braun, Heimsath, Chappell, 2001, Geology, v.29, pg. 683-686

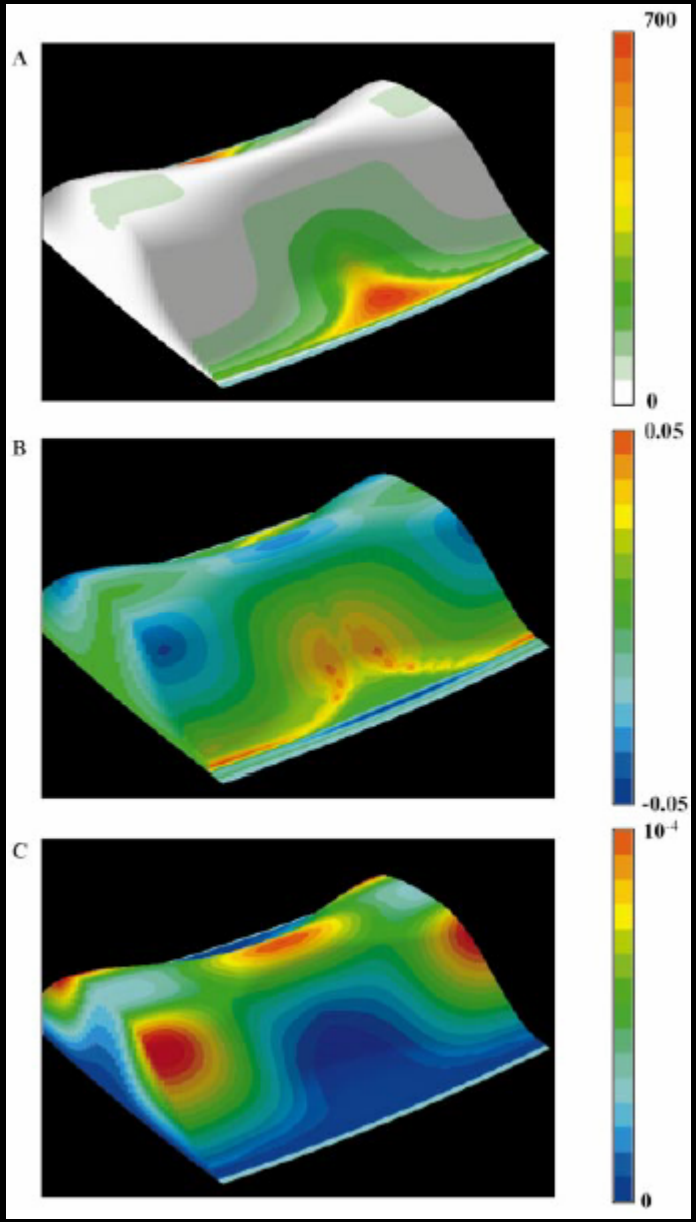

soil depth

Steady State Condition

curvature

soil production rate

Figure 1. Results of model after 100 k.y., in form of (A) soil thickness (in centimeters), (B) surface curvature (per meter) calculated at resolution of numerical grid (10 m), and (C) soil production rate (in meters per year). Transport parameter values (see text) are: $K_D = 3 \times 10^{-3}$ m^2·yr^{-1}, $K_v = 3 \times 10^{-3}$ m^{2-m}·yr^{-1}, $K_W = 3 \times 10^{-9}$ m^{2-3k}·yr^{k-1}, $m = 1.67$, $n = 0.5$, $k = 1.67$, $p = 1.3$, $P_0 = 53 \times 10^{-6}$ m·yr^{-1}, $h_0 = 0.5$ m. The precipitation rate is assumed to be uniform at 0.5 m·yr^{-1} · κ; the ratio of soil to bedrock density is 0.5. The time step used in the explicit time integration is 10 yr.

Braun, Heimsath, Chappell, 2001, Geology, v.29, pg. 683-686

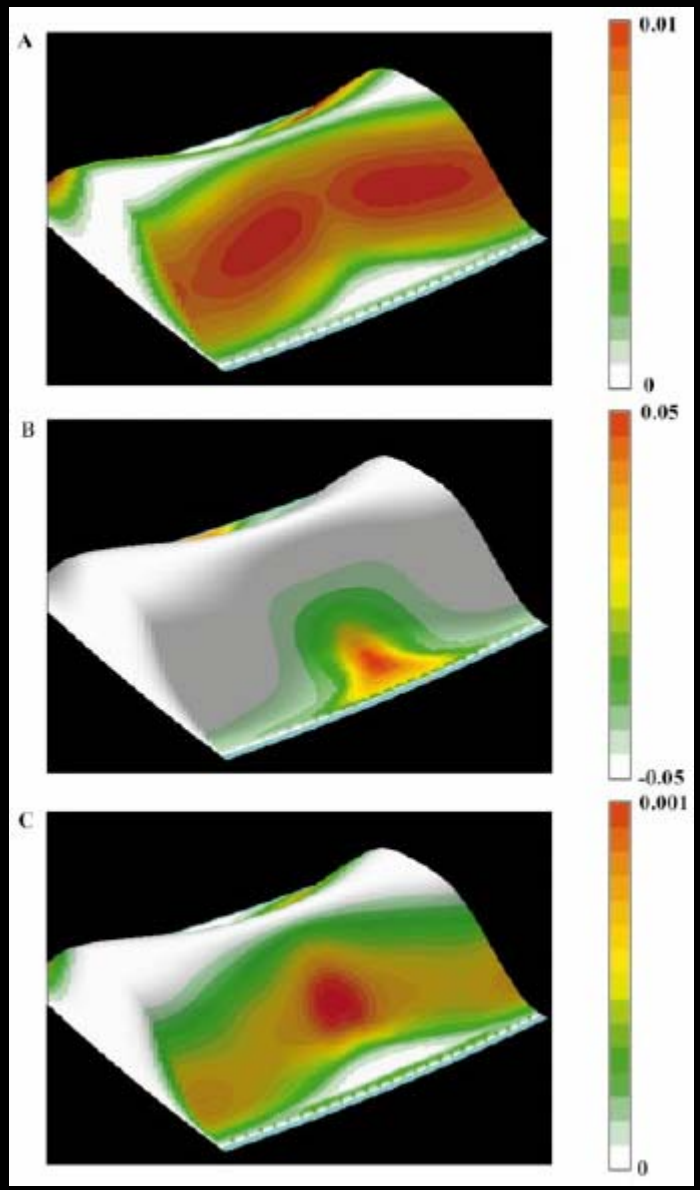

qs – linear creep

qs – rheologic creep

qs -- sheetwash

Figure 2. Contributions to total local soil flux (in $m^2 \cdot yr^{-1}$) from (A) linear creep, (B) depth-dependent creep, and (C) overland flow as computed by model after 100 k.y. Parameters are same as for Figure 1.

Braun, Heimsath, Chappell, 2001, Geology, v.29, pg. 683-686

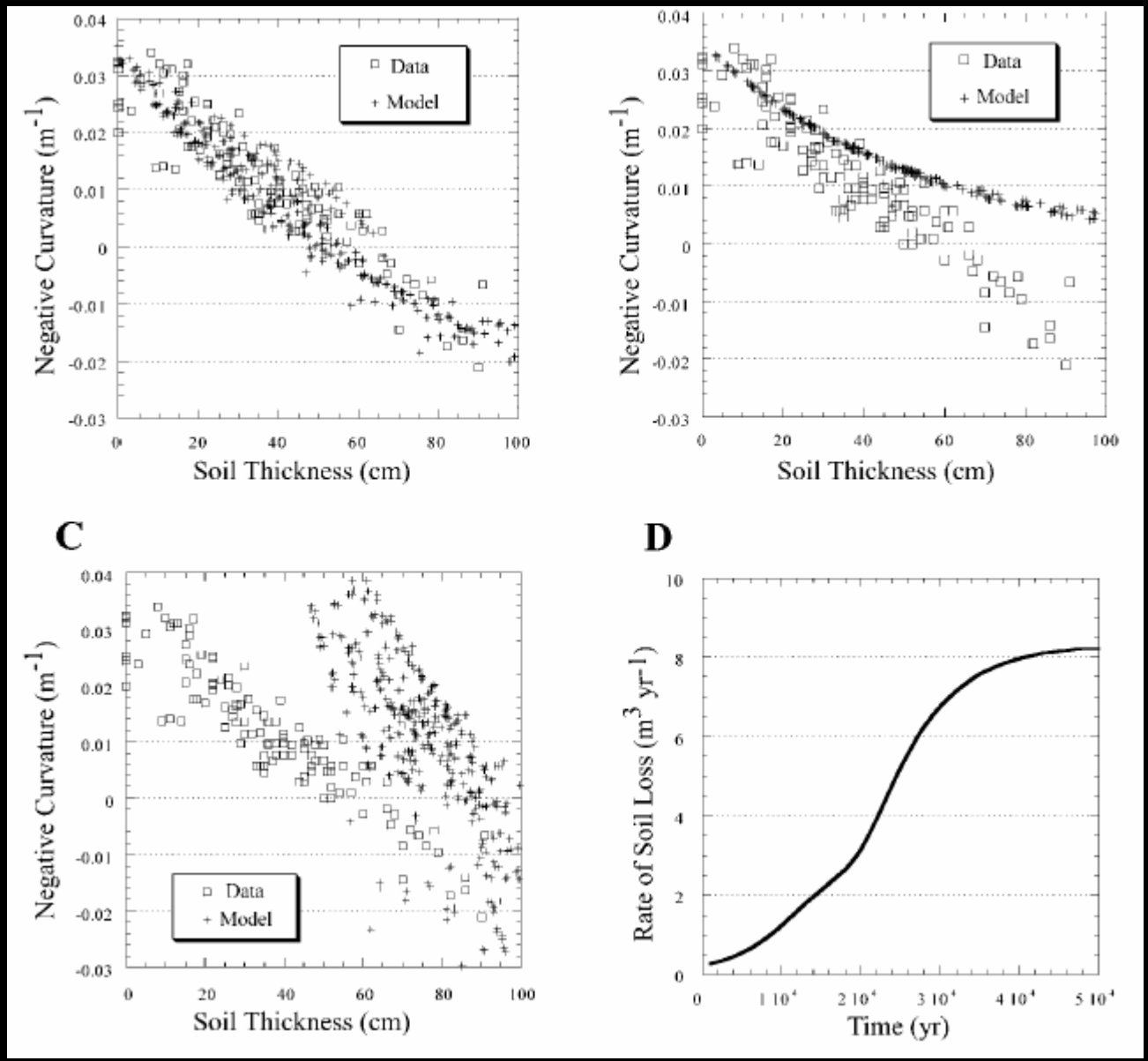

Figure 3. Computed curvature-thickness curves compared to observations at Bega Valley site (Heimsath et al., 2000) by using (A) model parameters given in Figure 1 caption (see text), (B) with K_v and K_w both set to zero, and (C) K_D and K_w set to zero. Rate of soil loss through upper and lower open boundaries is given in D for set of parameters given in Figure 1 caption.

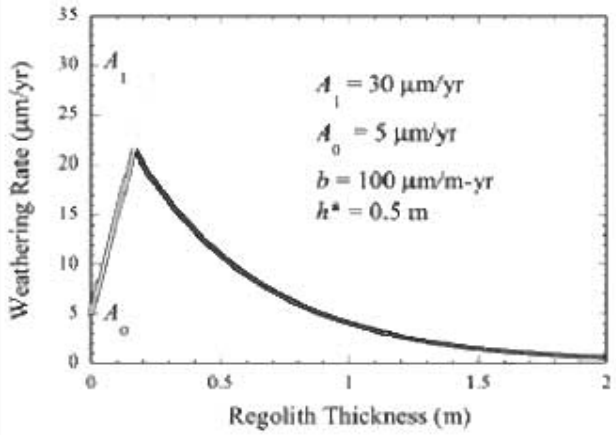

Fig. 7. Weathering rate dependence on regolith thickness, as used in the numerical model. Note linear increase of weathering with regolith thickness for thin regolith, and exponential decay after intersection with exponential function (here, -0.2 m).

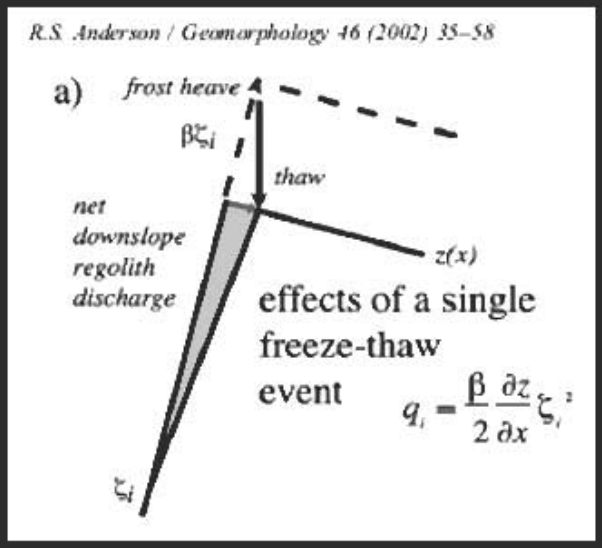
R.S. Anderson / Geomorphology 46 (2002) 35–58
a)
frost heave
$\beta\zeta_i$
thaw
net downslope regolith discharge
z(x)
effects of a single freeze-thaw event
$q_i = \frac{\beta}{2}\frac{\partial z}{\partial x}\zeta_i^2$
ζ_i

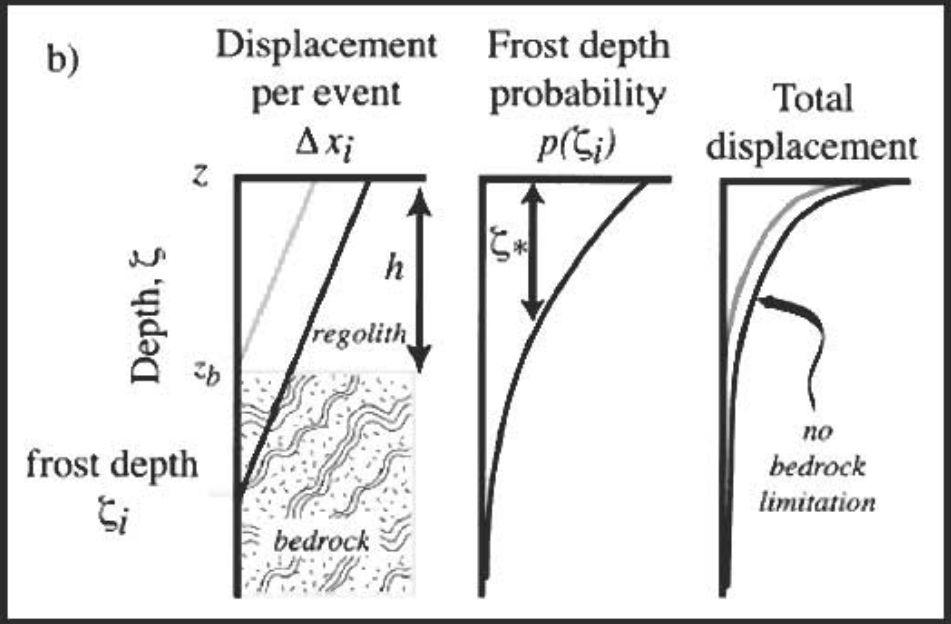
b)
Displacement per event
Δx_i
Frost depth probability
$p(\zeta_i)$
Total displacement
z
Depth, ζ
h
regolith
z_b
frost depth
ζ_i
bedrock
ζ_*
no bedrock limitation

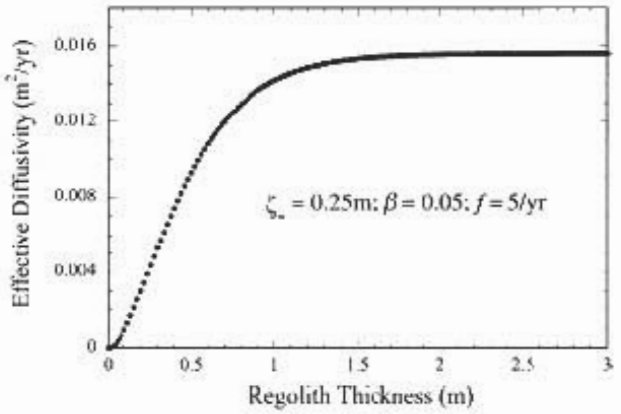

Fig. 9. Effective diffusivity (transport rate/local slope) as a function of regolith thickness on a specified slope (Eq. (19)), for specified values of depth scale for frost penetration, ζ_*, strain parameter, β, and frost frequency, f. Transport vanishes over bare bedrock (regolith thickness = 0) and asymptotically approaches a value set by the local slope angle for thick regolith.

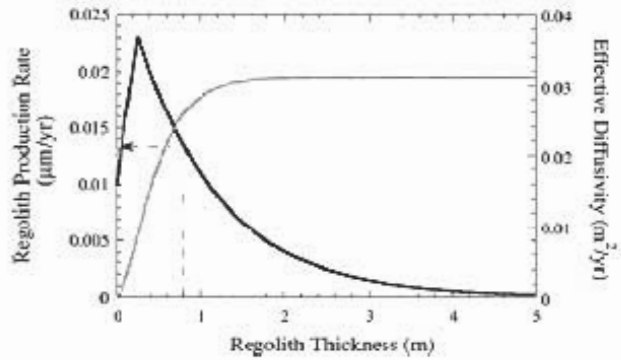

Fig. 11. Regolith production and effective diffusivity as functions of regolith thickness. Arrows denote final steady-state (uniform) regolith thickness (Fig. 12). Note that at this thickness the bare bedrock edge and the regolith-mantled surface are being lowered at roughly the same rates. In addition, the transport efficiency is approximately 90% of its asymptotic value.

Quantification of soil production and downslope creep rates from cosmogenic ^{10}Be accumulations on a hillslope profile

GEOLOGY, v. 21, p. 343–346, April 1993

James A. McKean
William E. Dietrich
Department of Geology and Geophysics, University of California, Berkeley, California 94720

Robert C. Finkel
John R. Southon
Marc W. Caffee
Center for Accelerator Mass Spectrometry, Lawrence Livermore National Laboratory, Livermore, California 94550

$$\int_0^x P_{Be}(x)\,dx = \int_0^h \rho_s(x,z)V_s(x,z)e_{Be}(x,z)\,dz.$$

$$Q_s(x) = \frac{P_{Be}x}{\rho_s C_{Be}(x)}.$$

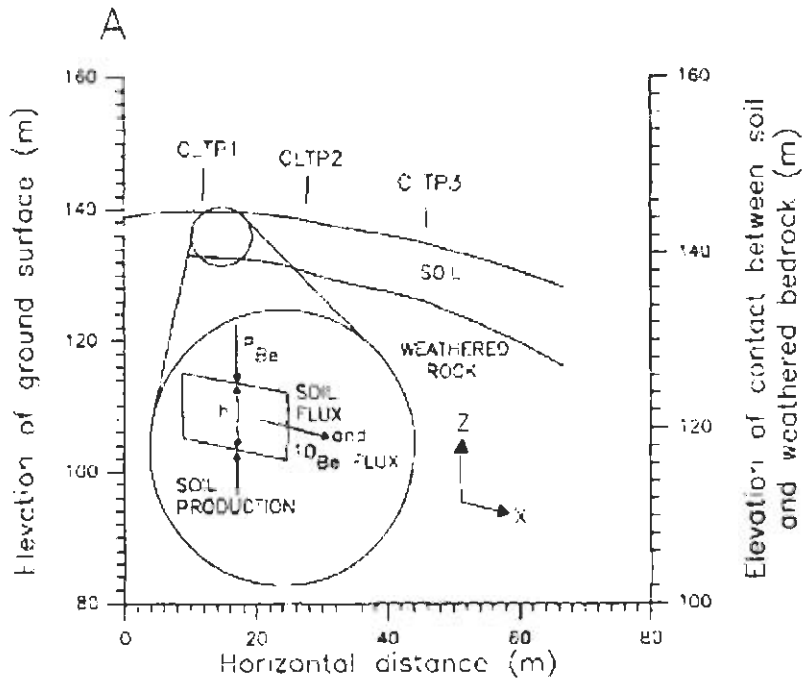

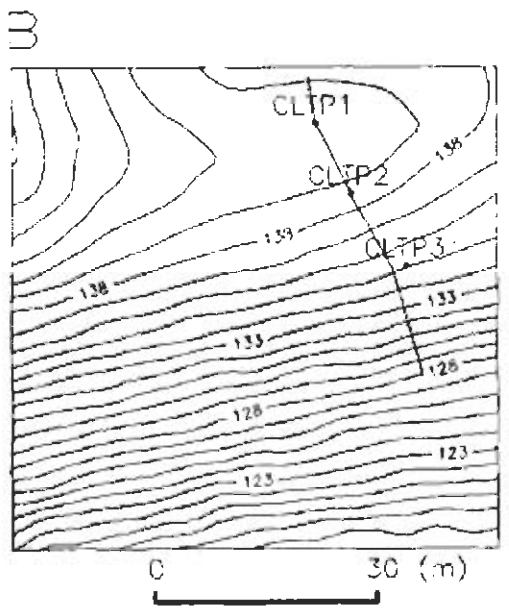

Figure 1. A: Hillslope profile (see B for location) with soil horizon defined on vertically exaggerated right-hand depth scale. Inset figure shows ^{10}Be and soil mass balance over some slope profile length interval x. P_{Be} = hillslope ^{10}Be deposition rate; soil creep mass flux = $\rho_s V_s h$; ^{10}Be mass flux = $C_{Be}\rho_s V_s h$; and soil production rate = $\rho_r C_r$. B: Black Diamond site topography. CLTP1, CLTP2, and CLTP3 are ^{10}Be sample locations on slope profile. Contour interval = 1 m. Scale bar = 30 m.

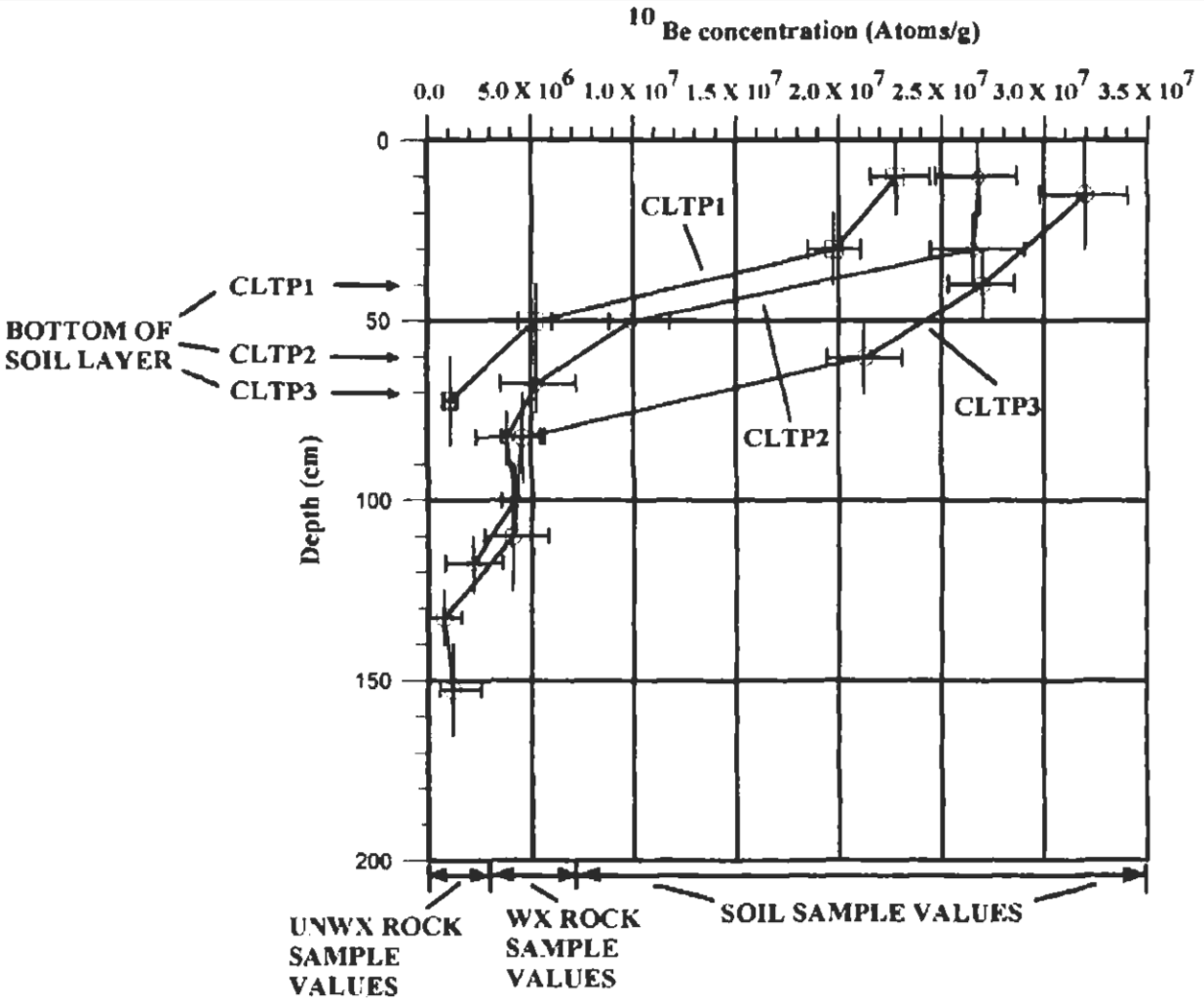

Figure 2. Profiles of ^{10}Be concentration in test pits, Black Diamond Mines Regional Preserve. Vertical lines through data points represent sample depth intervals. Each data point is average of two duplicate measurements. Error bars represent maximum and minimum AMS 1 σ uncertainty values for two duplicate samples. WX = weathered bedrock and UNWX = unweathered bedrock. Bottom of soil horizon in each test pit noted on vertical axis.

$$Q_s(x) = \frac{P_{Be} x}{\rho_s C_{Be}(x)}.$$

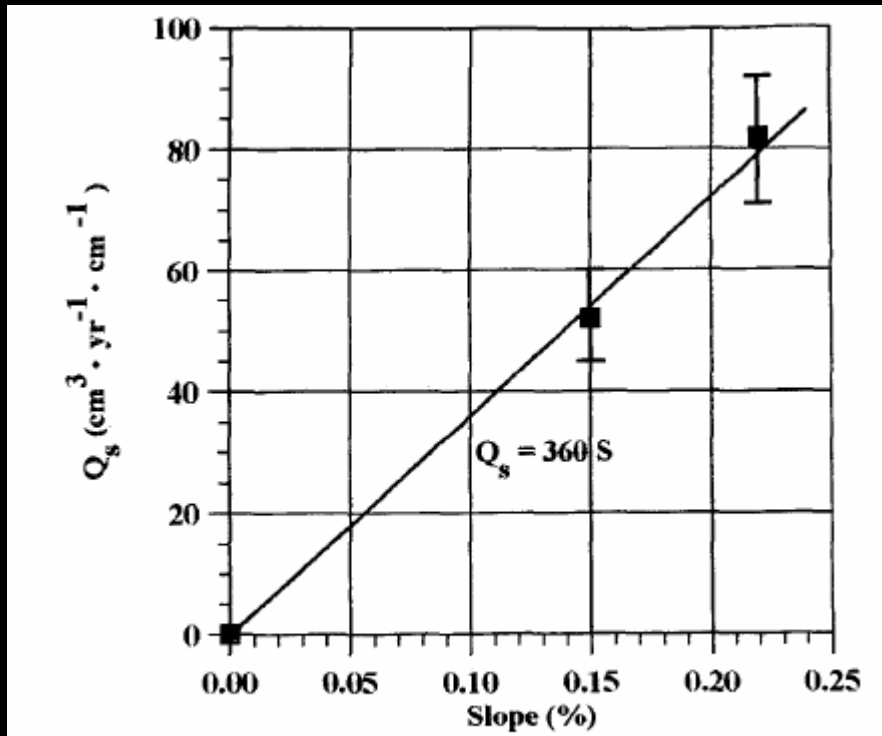

Figure 3. Slope vs. soil-creep flux rate (Q_s). S = ground surface percent slope. Error bars indicate ~15% uncertainty in technique.

Confirmation Qs linear with Slope (over this range of shallow slopes); but
No direct test of (a) non-linearity at high slopes, (b) dependence on soil depth